

Multiple Site-specific Infrared Dichroism of CD3- ζ , a Transmembrane Helix Bundle

Jaume Torres¹, John A. G. Briggs² and Isaiah T. Arkin^{3*}

¹Cambridge Centre for Molecular Recognition
Department of Biochemistry
University of Cambridge, 80
Tennis Court Road, Cambridge
CB2 1GA, UK

²Department of Biochemistry
University of Oxford, South
Parks Road, Oxford, OX1 3QU
UK

³The Alexander Silberman
Institute of Life Sciences
Department of Biological
Chemistry, The Hebrew
University, Givat-Ram
Jerusalem 91904, Israel

The structure of the transmembrane domain of CD3- ζ a component of the T-cell receptor involved in signal transduction, has been studied in its native state (a lipid bilayer) by multiple site-specific infrared dichroism. For the first time, the transmembrane domain has been labelled at multiple positions along the sequence, representing a total of 11 samples, each labelled at a different residue with an isotopically modified carbonyl group, $^{13}\text{C}=\text{O}$. A strategy is outlined that, based on the above data, can yield the rotational orientation and the local helix tilt for each labelled residue, giving a detailed description of helix geometry. The results obtained indicate that the transmembrane segment is in an α -helical conformation throughout, with an average helix tilt of 12° . The N-terminal side of the helix is more tilted than the C-terminal.

In an accompanying paper we describe the implementation of the infrared data in a model-building study of the CD3- ζ transmembrane complex. The model obtained is entirely consistent with results based on evolutionary conservation data. Taken together, this study represents the first step towards elucidation of the backbone structure of a transmembrane α -helical bundle by infrared spectroscopy.

© 2002 Elsevier Science Ltd.

Keywords: membrane proteins; molecular dynamics; molecular modelling; site-specific infrared dichroism; CD3- ζ

*Corresponding author

Introduction

Structural biology of membrane proteins is plagued by the paucity of experimental data. This is due to the known difficulties that conventional methods used for structural elucidation (i.e. X-ray crystallography and solution NMR spectroscopy)

encounter when applied to membrane proteins. Since membrane proteins are genomically abundant,¹ and far more biomedically important than their water-soluble counterparts†, the need to develop alternative structural methods, applicable to membrane proteins, cannot be overstated. We have recently shown that site-specific infrared dichroism (SSID) has the potential of becoming such a method.²

Present address: J. Torres, School of Biological Sciences, Nanyang Technological University, Block 5 Level 3, 637616 Singapore.

Abbreviations used: FTIR, Fourier transform infrared spectroscopy; ATR, attenuated total internal reflection; RMSD, root-mean-square deviation; CNS, Crystallography & NMR System; CHI, CNS searching of helix interactions; Fmoc, 9-fluorenylmethoxycarbonyl; HFIP, hexafluoroisopropanol; DMPC, 1,2-dimyristoyl-*sn*-glycero-3-phosphocholine; TFA, trifluoroacetic acid; SSID, site-specific infrared dichroism.

The method is based on the measurement of dichroism arising from site-specific isotopic labels, e.g. $1\text{-}^{13}\text{C}=\text{O}$,³ or C-deuterated glycine,⁴ to yield accurate spatial restraints that can describe the structure of small membrane proteins in their native environment, a lipid bilayer. In theory, SSID can yield spatial restraints for a protein of any size, but realistically it is exceedingly difficult to insert an isotopic label selectively into a large membrane protein. We overcome the problem of deconvoluting the disorder in the sample through the use of more than one observable on the helix, the helix dichroism and the isotopic site-specific dichroism. Since both observables are present on the same molecule, they share the same disorder. With the use of one more sample, in which the isotopic label is located at a different position, it is possible to

† The reason for paramount biomedical importance of membrane proteins lies in the fact that they serve as targets for the vast majority of pharmaceutical agents in current use.

E-mail address of the corresponding author: arkin@cc.huji.ac.il

obtain the average helix tilt and the rotational pitch angle of the labeled site (see Figure 5).² This is possible only upon knowledge of the rotational pitch angle difference between the two labelled sites. In a canonical helix it would simply be 100° for consecutive residues.

This assumption has been employed in previous applications of SSID, where we have used only one pair of isotopically labeled carbonyls, either $1\text{-}^{13}\text{C}=\text{O}$ in *Influenza* M2 and CM2, or vpu from HIV⁵⁻⁷ or the double-isotope $1\text{-}^{13}\text{C}=\text{O}$ in phospholamban,³ to obtain the average helix tilt and rotational pitch angle of the labeled amino acid. In an effort to better characterize a transmembrane helix bundle, in the present study we have employed, for the first time, multiple $1\text{-}^{13}\text{C}=\text{O}$ labels,^{5,8} which allows gathering of information at different points along the helix and makes unnecessary the assumption referred to above.

We have applied this new approach to the CD3- ζ chain, one of the invariant subunits of the T-cell receptor (TCR). CD3- ζ is a glycoprotein essential for TCR expression, incorporated as the final and rate-limiting step in the assembly of the TCR complex^{9,10} and is involved in signal transduction.¹¹ The human CD3- ζ chain is 163 residues long and spans the membrane once (residues 31-51). SDS-PAGE analysis indicates that CD3- ζ forms disulphide-linked dimers under these denaturing conditions, and that the two monomers associate through their transmembrane domains.¹² Furthermore, it has been hypothesized that the transmembrane domain of CD3- ζ contains a glycine-based dimerization motif similar to that of glycoporphin A (gpA).¹³

We show that isotopic multiple labelling of a transmembrane α -helical bundle allows a more accurate description of the orientation of the helix, as the information is gathered at different points along its length. Thus, the current study represents the first example in which SSID is used to derive comprehensive site-specific spatial restraints.

Results and Discussion

Effect of hydration

We have used, as is usual practice,^{3,5} data from samples in which excess water was removed, since it is difficult to measure the site dichroism from a fully hydrated sample because both H_2O and $^2\text{H}_2\text{O}$ affect the band corresponding to the $^{13}\text{C}=\text{O}$ label. The bending O- ^2H vibration of $^2\text{H}_2\text{O}$ absorbs in the same region as the label $^{13}\text{C}=\text{O}$, at 1590 cm^{-1} (not shown), whereas H_2O absorbs strongly in the amide I region, affecting the $^{13}\text{C}=\text{O}$ band. However, as described in Materials and Methods, we have monitored the effect of hydration on the structure of the protein by comparing the amide A dichroism before and after excess water removal (nine samples), as shown in Figure 1.

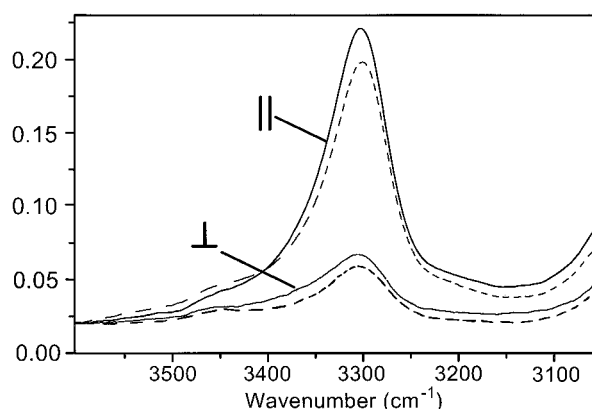


Figure 1. Amide A region of a sample fully hydrated in $^2\text{H}_2\text{O}$ (broken line) and after removing excess $^2\text{H}_2\text{O}$ (continuous line). The intensity of the band for the hydrated sample is lower due to swelling upon hydration. The polarization of light is indicated.

The average dichroisms were 4.50 ± 0.71 and 4.28 ± 0.57 , for samples with or without excess water, respectively. The difference in dichroism, however, accounts for a change in helix tilt of only 1.5° (using 29° as the angle between the N-H stretching transition dipole moment and the helix axis^{16,17}), well within the error of the measured helix tilt (see Table 2). Therefore, we can conclude that the removal of excess water does not affect the structure of CD3- ζ significantly.

Finally, dichroism of the lipid CH_2 stretching modes (ca 2924 and 2852 cm^{-1} , data not shown) was not affected by the changes of hydration. Order parameters calculated from the above modes were routinely above 0.5, indicative of well-formed, parallel multi-bilayers.

Multiple site-specific infrared dichroism of CD3- ζ

Figure 2 shows representative amide I spectra for each of the 11 peptides labelled, at parallel and perpendicular polarizations. The bands arising from the $1\text{-}^{13}\text{C}=\text{O}$ -labelled residue are also shown.

All 66 spectra (six for each label) were typical of a predominantly α -helical peptide, with an amide I band with a maximum at 1657 cm^{-1} .¹⁹ Neither the original nor the deconvoluted (not shown) spectra show significant intensity around $1640\text{-}1630\text{ cm}^{-1}$, indicating the absence of significant β structure.¹⁹ This result indicates that the transmembrane segments of the proteins in the regions analyzed (34L-49L) is entirely α -helical. Of these spectra, only the 33 samples (three for each label) containing less disorder, i.e. f more than 0.8, were used for the calculations of β and ω . The recorded dichroic ratios for these 33 samples, $\mathcal{R}_{\text{Helix}}$ and $\mathcal{R}_{\text{site}}$, are listed in Table 1.

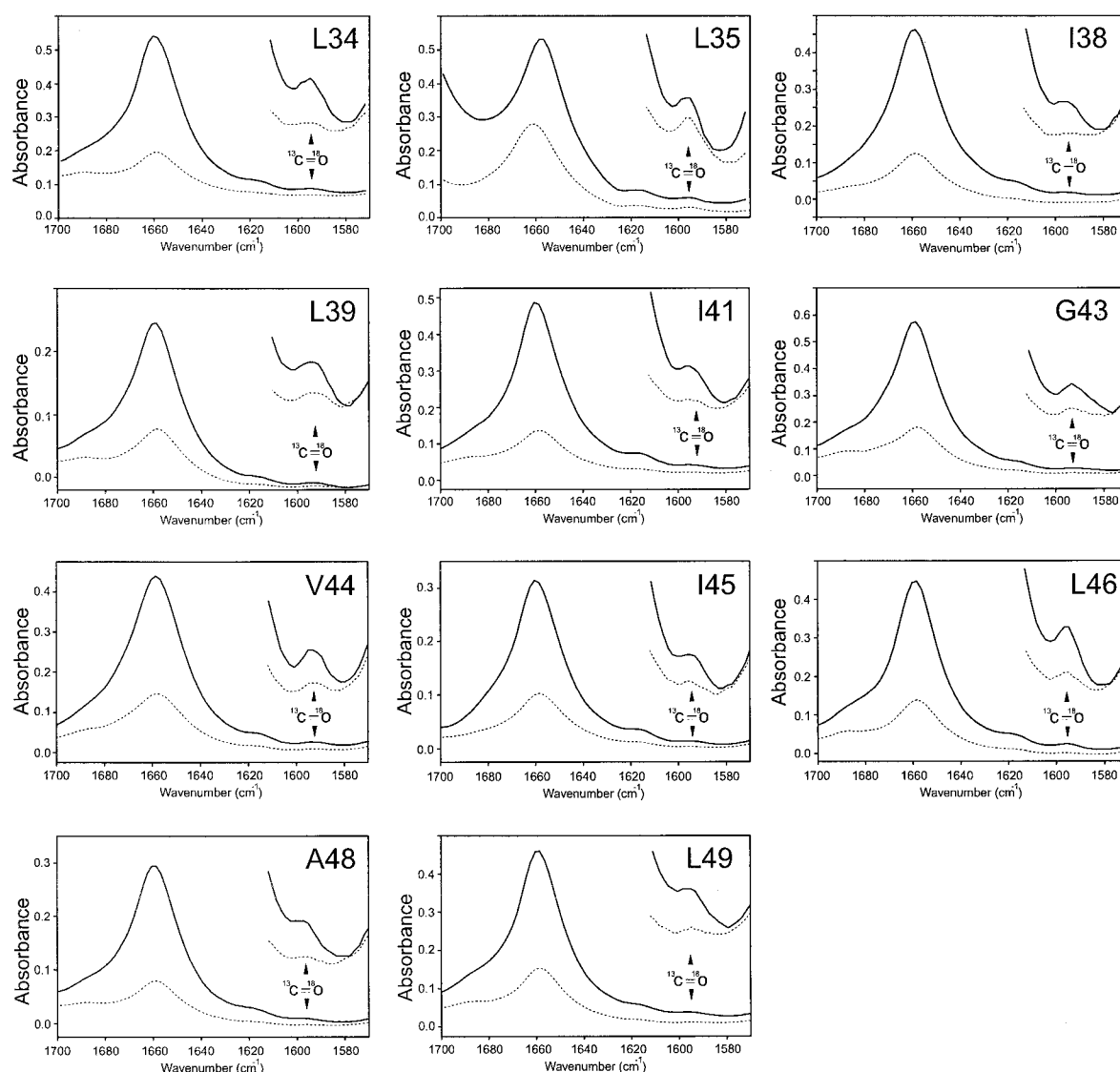


Figure 2. ATR-FTIR spectra corresponding to the amide I region of the transmembrane domain of CD3- ζ obtained with parallel (continuous line) or perpendicular (dotted line) polarized light. The position of the band arising from the $^{13}\text{C}=\text{}^{18}\text{O}$ label is indicated. The inserts show the bands corresponding to the $1\text{-}^{13}\text{C}=\text{}^{18}\text{O}$ label, centered at 1590 cm^{-1} . The residue labelled in each case is indicated at the top right-hand corner.

From the dichroisms in Table 1, the values for the local helix tilt β and rotational orientation ω for every labelled residue were calculated (see Materials and Methods). These parameters are shown in the first two columns of Table 2. From the values shown in this Table, it is clear that the tilt obtained from residues 34 to 38 is higher than the tilt obtained from residue 41 to 49, which suggests the presence of a kink or bend in the helix.

Inspection of the rotational pitch angle determined, (Figure 3, top panel) illustrates that deviations from a canonical helix (Figure 3, bottom panel) are not substantial. In line with the change in local helix tilt observed between residues 39L and 41I, a concomitant deviation from canonical helix increments is observed. Likewise, smaller

deviations in increment are observed whenever changes in helix tilt are observed (e.g. 34-35 and 46-45).

Comparison with previous modeling results

We then compared these results with the calculated ω and β angles of the “glycophorin-like” right-handed dimeric model we reported previously¹⁵ (see Table 2, last two columns). Surprisingly, our experimental data are not compatible with that model.

There is, however, a general agreement with another dimeric model that is produced from global searching molecular dynamics simulations ($\omega_{\text{V44}} \sim 230^\circ$) but was not identified as the native model.¹⁵ This alternative dimeric model (Figure 4,

Table 1. Helix and site dichroisms obtained for each one of the samples analysed

Residue	$\mathcal{R}_{\text{HELIX}}$	$\mathcal{R}_{\text{C=O}}$
34L _a	3.99	4.75
34L _b	2.76	3.20
34L _c	3.37	2.87
35L _a	3.79	7.66
35L _b	3.33	6.24
35L _c	3.61	6.65
38I _a	3.65	4.38
38I _b	3.50	3.59
38I _c	3.48	4.40
39I _a	3.28	2.41
39I _b	3.06	2.24
39I _c	3.41	2.83
41I _a	3.53	3.71
41I _b	4.35	3.91
41I _c	4.17	3.90
43G _a	3.61	2.93
43G _b	4.00	3.57
43G _c	3.50	3.18
44V _a	3.88	2.87
44V _b	3.46	2.80
44V _c	3.41	2.52
44V _d	3.06	2.63
45I _a	2.95	3.58
45I _b	3.22	3.77
45I _c	2.91	3.51
46L _a	3.03	3.44
46L _b	3.23	3.49
46L _c	2.95	3.22
48A _a	3.90	2.91
48A _b	3.93	3.03
48A _c	4.28	3.02
49L _a	2.70	3.30
49L _b	3.30	5.11
49L _c	3.25	3.83

Only three of the best measurements (see Materials and Methods) are represented for each labelled site, out of six typically measured. Variability within each sample represents variability in sample order.

left panel), however, is incompatible with a number of observations in the literature. For example, the aspartic residue D36, essential for

dimerization,¹² is facing the exterior of the dimer. Other residues that have been identified as pertaining to a dimerizing motif¹³ (e.g. G33, V44 and T47) are facing the exterior of the dimer. In contrast, in the structure corresponding to the glycoporphin-like model reported previously ($\omega_{\text{V44}} = 350^\circ$) (Figure 4, right panel), these residues are all involved in inter-helical interactions. Thus, it seems unlikely that dimers are forming with the residues that were characterized previously as important for dimerization facing the outside of the dimer.

Another possible explanation for this inconsistency is that the sample is not homogeneous with respect to oligomerization. However, the results consistently converge to a certain solution with physically possible helix tilts and f values, i.e. between 0 and 1. Also, the increment in ω between consecutive residues is roughly 100° . This indicates that the sample is homogeneous with respect to oligomerization, i.e. a vastly predominant species must exist to account for the consistency of the data.

Therefore, a far more satisfactory interpretation of the data arises when the possibility of higher-order oligomers is considered. This possibility is explored in the accompanying paper.²⁰

Conclusion

We have, for the first time, employed multiple site-specific infrared dichroism to analyze the structure of a transmembrane α -helical bundle. Using 11 labels in the transmembrane domain, we were able to obtain local helix tilts as well as the rotational pitch angles for each of the labels. The results indicate that there is a change in helix tilt in the helix. Thus, the work represents the first stage in employing an entirely novel method to solve the backbone structure of a transmembrane α -helix under native conditions.

Table 2. Orientational parameters ω and β for the labelled residues of CD- ζ incorporated in a lipid bilayer

Residue	Sample size	$\omega_{\text{experimental}}$ (deg.)	$\beta_{\text{experimental}}$ (deg.)	$\Delta\omega$	ω_{dimer} (deg.)	β_{dimer} (deg.)
34L	3	295 \pm 6	14 \pm 2	87	74	13
35L	3	22 \pm 5	20 \pm 2	93	176	9
38I	3	300 \pm 10	19 \pm 5	170	88	12
39L	3	110 \pm 5	19 \pm 6	85	160	9
41I	3	280 \pm 12	7 \pm 2	100	36	15
43G	3	120 \pm 9	8 \pm 1	104	260	12
44V	3	224 \pm 11	8 \pm 1	106	350	19
45I	4	330 \pm 6	8 \pm 1	107	73	18
46L	3	77 \pm 10	12 \pm 2	79	174	13
48A	3	234 \pm 14	9 \pm 2	108	18	13
49L	3	342 \pm 30	-	-	112	13

Sample size is the number of samples incorporated in the data (see Materials and Methods). The difference in the rotational pitch angle between adjacent residues $\Delta\omega$ is listed in the fifth column. When a gap is present between the labels (e.g. 35L and 38I) the difference is calculated as an average over the gap size (e.g. 35L and 38I $\Delta\omega = (300-22)/3 = 93$). The last two columns indicate the values for these parameters for the dimeric model we reported previously.¹⁵

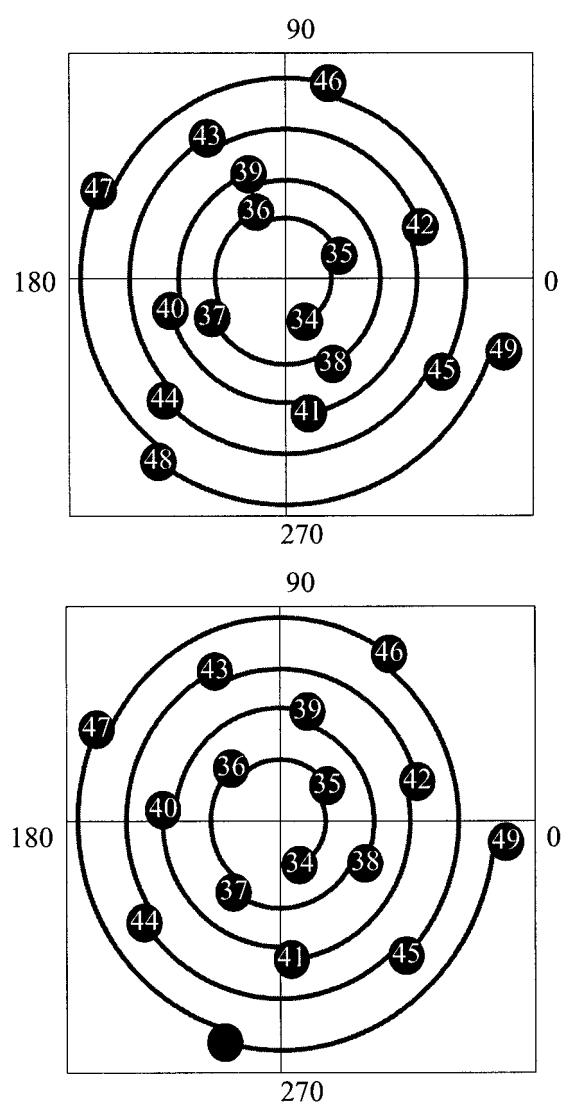


Figure 3. Top: Helical wheel projection of the rotational pitch angles obtained in the experiment (see Table 2). When a gap in the label placements exists, (e.g. between 35L and 38L) the difference in ω are an average of the difference divided by the $\Delta\omega$ obtained. Average residues are colored in red. Bottom: A helical wheel projection of a canonical helix (100° difference between adjacent amino acid residues).

Materials and Methods

Isotopic labelling and peptide synthesis

Amino acids labelled with a double isotope, $^{13}\text{C}=^{18}\text{O}$,^{3,8} were obtained by incubating the [^{13}C]carboxyl-containing amino acids, $^{13}\text{C}=^{16}\text{O}$ (Cambridge Isotopes Laboratories, Andover, MA), with a mixture of H_2^{18}O (94.4% Promochem GmbH) and dioxane (3:1, v/v) for one hour at 100°C at acidic pH (ca 1). The extent of $^{16}\text{O}/^{18}\text{O}$ exchange was monitored using mass spectrometry, and was typically $\sim 75\%$, i.e. 75% of the oxygen atoms in the carboxylic group of the amino acid. Therefore, 75% of the molecules of synthesized peptide

contained a $^{13}\text{C}=^{18}\text{O}$ -labelled residue. The fact that the exchange was not complete is not important, as the dichroism of the label is independent of its relative abundance in the sample. The mixture was lyophilized and the amino acid was derivatized with Fmoc as described.¹⁴

The transmembrane segment of CD3- ζ (residues 27 to 53) was synthesized by standard solid-phase Fmoc chemistry, cleaved from the resin with trifluoroacetic acid and lyophilized. As in the simulations reported previously,¹⁵ a transmembrane sequence with the mutation C32G was employed (see Figure 5, bottom), because it facilitates both peptide purification and molecular dynamics simulations and has no influence on TCR expression.¹³ During the synthesis of the peptide, residues with a $^{13}\text{C}=^{18}\text{O}$ -labelled carbonyl group were introduced at positions L34, L35, I38, L39, I41, G43, V44, I45, L46, A48 or L49, so that 11 different samples were obtained, each labelled at a different residue (see Figure 5).

The lyophilized peptides were dissolved in 2 ml of trifluoroacetic acid (TFA) (final concentration ca 5 mg/ml) and immediately injected onto a 20 ml Juppiter 5 C4-300 Å column (Phenomenex, Cheshire, UK) equilibrated with 95% H_2O , 2% (w/v) acetonitrile and 3% (v/v) 2-propanol. Peptide elution was achieved with a linear gradient to a final solvent composition of 5% H_2O , 38% acetonitrile and 57% 2-propanol (Biocad Sprint, Perceptive Biosystems, Cambridge, USA). All solvents contained 0.1% (v/v) TFA. The resulting fractions were pooled and lyophilized. Peptide purity was confirmed by mass spectrometry.

Sample preparation for ATR-FTIR

Initially, 100 μl of a stock solution of DMPC in HFIP (100 mg/ml) were added to the dry peptide (typically ~ 3 mg). The lipid-to-protein ratio was checked using a CaF window in transmission mode, drying a 10 μl aliquot on the window surface. If the intensity of the ester band of the lipid (at 1740 cm^{-1}) was smaller than the amide I, additional HFIP/lipid solution was added. Then, the sample was diluted with a further 900 μl of HFIP, to a final DMPC concentration of 10 mg/ml ($>15:1$ DMPC/peptide molar ratio) and approximately 100 μl of this solution were deposited, in successive aliquots of 10 μl , onto a trapezoidal (50 mm \times 2 mm \times 20 mm) Ge internal reflection element.

At this point, immediately after evaporating the HFIP, the dry sample was oriented randomly (the amide I dichroism was ~ 2),² but the dichroism of the amide I increased (up to typically 3 to 4) after hydrating the sample with nitrogen saturated with H_2O , or $^2\text{H}_2\text{O}$ for 30 minutes, after which no further increase in the helix dichroism was observed. After hydration, excess water was removed using a dry N_2 stream through the ATR compartment and spectra were collected.

Data collection and area integration

FTIR spectra were recorded on a Nicolet Magna 560 spectrometer (Madison, USA) purged with N_2 and equipped with a MCT/A detector, cooled with liquid nitrogen. Attenuated total reflection (ATR) spectra were measured with a 25 reflections ATR accessory from Graseby Specac (Kent, UK) and a wire grid polarizer (0.25 μm , Graseby Specac). A total of 1000 interferograms collected at a resolution of 4 cm^{-1} were averaged for

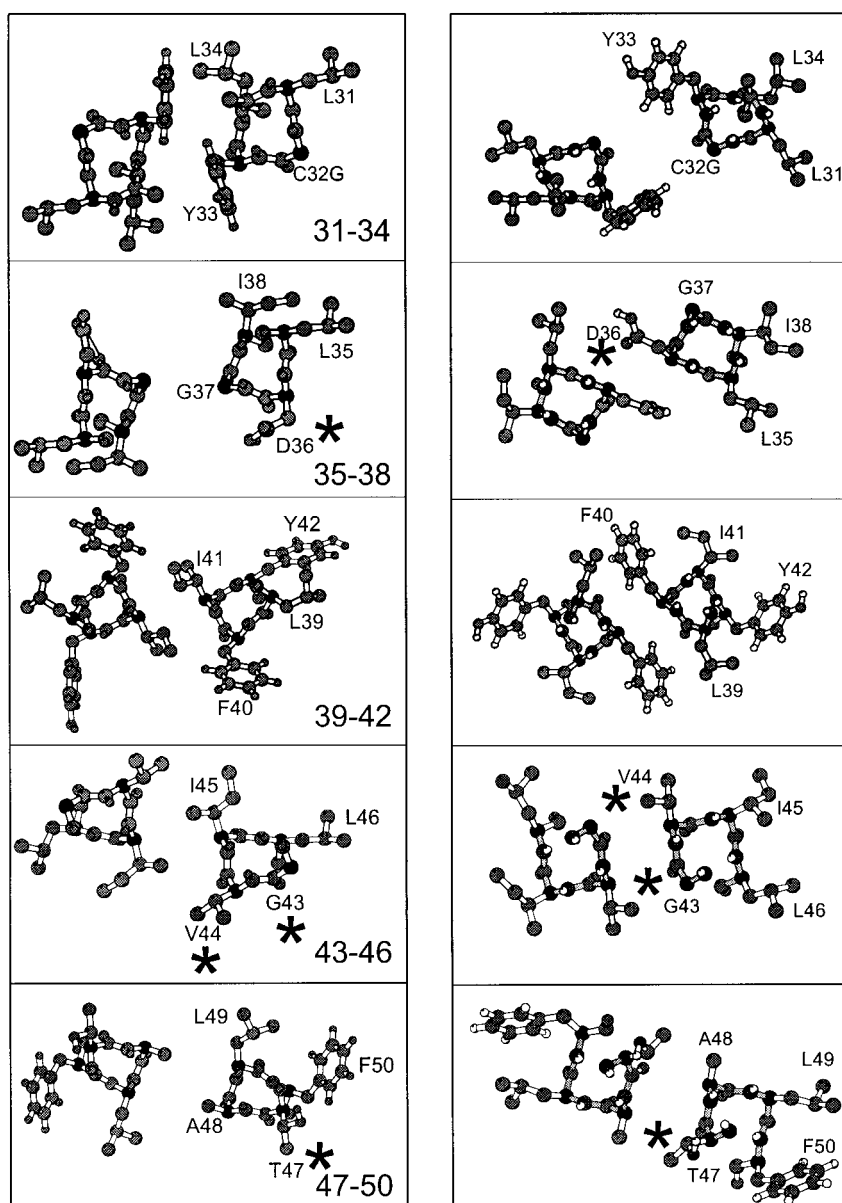


Figure 4. Ball-and-stick representation of slices through the CD3- ζ homodimer in the model in agreement with the data, with $\omega_{V44} = 224^\circ$ (left panel) and the model we reported previously,¹⁵ with $\omega_{V44} = 340^\circ$ (right panel). The atoms are represented at 0.25 of the Van der Waals radii. The residues important for dimerization¹³ are indicated by a star. The C $^\alpha$ atoms are black and hydrogen atoms are white. Non polar hydrogen atoms are not represented. The molecular graphics were generated with MOLSCRIPT.²¹

every sample and processed with one point zero filling and Happ-Genzel apodization.

The area corresponding to the $^{13}\text{C}=\text{O}$ (isotope-labelled) carbonyl stretching vibration was obtained by integrating the band at 1590 cm^{-1} between 1600 cm^{-1} and 1580 cm^{-1} .^{3,8} The area of the amide I, corresponding to helical structure, was obtained by peak integration from 1670 to 1645 cm^{-1} . The area of the amide A was calculated by integrating the band centered at $\sim 3300\text{ cm}^{-1}$ between 3200 and 3400 cm^{-1} .

The dichroic ratios were calculated as the ratio between the integrated absorptions of the spectra collected with parallel and perpendicular polarized light.

Effect of hydration

The effect of hydration on the helix dichroism was assessed by monitoring the dichroism of the amide A

band (due to N-H stretching), centered at $\sim 3300\text{ cm}^{-1}$, in different states of $^2\text{H}_2\text{O}$ hydration. The reason for studying hydration with $^2\text{H}_2\text{O}$, stems from the overlap of the O-H stretching modes of H_2O in the amide A region. The comparison of spectra before and after removal of excess $^2\text{H}_2\text{O}$ was conducted as follows. First, the spectra of the hydrated sample were collected after flushing the sample with $^2\text{H}_2\text{O}$ -saturated N_2 . Then, spectra were collected after excess water was removed from this sample as described above.

Multiple site-specific infrared dichroism

The data were analyzed according to the theory of SSID presented in detail elsewhere.² Briefly, SSID is based on the fact that the measured dichroism, \mathcal{R} , of a particular transition dipole moment is a function of the sample fractional order, f , and the spatial orientation of

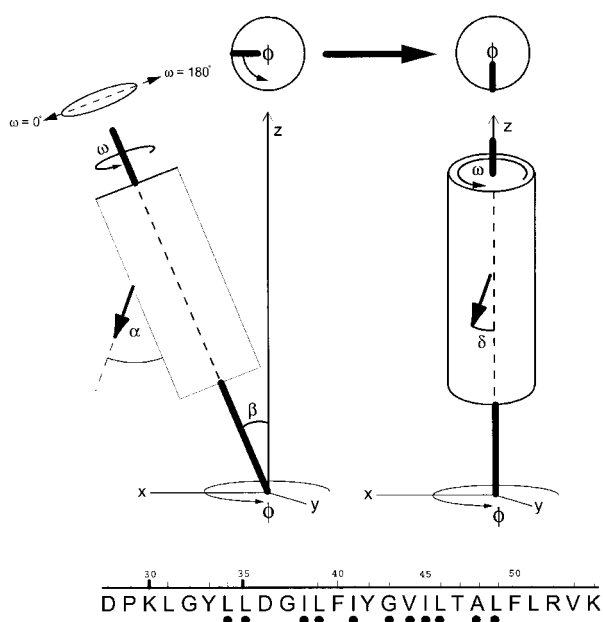


Figure 5. Top: Drawing representing the geometric parameters that define the orientation of a bond or a transition dipole moment in a transmembrane helix. The helix tilt β and the rotational orientation ω are derived from the experimental data using the angles α and δ which are known (see the text). The helix presents axial symmetry around the z -axis, i.e. all possible ϕ angles are present. The helical segment has been drawn as a perfect cylinder for simplicity. Bottom: Transmembrane sequence of CD3- ζ , where the residues modified with $^{13}\text{C}=\text{O}$ are indicated with a black dot.

the dipole. The latter is defined by the parameters shown in Figure 5: β the helix tilt, α and δ , which relate the transition dipole moment to the helix director, and the rotational pitch angle, ω . The rotational pitch angle ω is arbitrarily defined as 0° in the direction of the helix tilt when the transition dipole moment, the helix director and the z -axis all reside in the same plane. The δ angle is defined by the angle between the transition dipole moment and the helix axis when the z -axis, the helix axis and the α -carbon atom of the residue are in the same plane (see Figure 5). The angles α and δ for the $\text{C}=\text{O}$ and $\text{N}-\text{H}$ transition dipole moments are known from studies using oriented fibers. The values for δ were 0° for both transition dipole moments, whereas α was 39° for $\text{C}=\text{O}$ and 29° for $\text{N}-\text{H}$.^{16,17}

From each measurement, two different dichroisms are obtained. The first is $\mathcal{R}_{\text{Helix}_i}$, the composite dichroism that corresponds to all the $^{12}\text{C}=\text{O}$ dipoles, or $\text{N}-\text{H}$ in the case of amide A, involved in the helical structure for sample i . This dichroism arises from residues distributed around the helical axis, i.e. one every 100° for a canonical α -helix. Therefore, this dichroism is independent of ω and dependent solely on β and f_i :

$$\mathcal{R}_{\text{Helix}_i}(\beta, f_i) = \frac{e_z^2 \left(f_i \mathcal{K}_z + \frac{1-f_i}{3} \right) + e_x^2 \left(f_i \mathcal{K}_x + \frac{1-f_i}{3} \right)}{e_y^2 \left(f_i \mathcal{K}_y + \frac{1-f_i}{3} \right)} \quad (1)$$

where $\mathcal{K}_{x,y \text{ or } z}(\omega)$ are the rotationally averaged, integrated absorption coefficients and f_i represents the fractional order of preparation i . The parameter f is 1 if the sample is completely ordered and zero if completely random. Finally, e_x , e_y and e_z are the electric field components for each axis given by Harrick.¹⁸ The values for these components were those corresponding to a thick film approximation because, whereas the thickness of the film was calculated as being more than $30 \mu\text{m}$, the amplitude of the evanescent wave decays (at $1/e$ of its initial value) after $1 \mu\text{m}$ in a germanium plate.

Instead of using the amide I dichroism, we obtained $\mathcal{R}_{\text{Helix}}$ by measuring the amide A dichroism when the sample was exposed to $^2\text{H}_2\text{O}$. The reasoning behind this experiment is twofold. (1) The sensitivity of a dichroism experiment depends on the magnitude of the α angle. The range of possible dichroic ratios is a function of α angle as shown in Figure 6. As an extreme example, when $\alpha = 54.6^\circ$ (the magic angle) the dichroic ratio is independent of the helix tilt. Clearly, the higher the range of possible dichroic ratios is, the more accurately the tilt can be determined. For example, the range of dichroic ratios for the amide I (in the Ge ATR optical configuration) is 1.4-4.6, while for the amide A it is 1.2-8.3. Thus, a helix tilt difference between 25 and 30° will be reflected in a change of dichroism of only 9% ($3.5 \rightarrow 3.2$) when observing the amide I mode, but a change of 16% ($5.1 \rightarrow 4.3$) when observing the amide A mode. Incidentally, it is immediately apparent from Figure 6 why it is difficult to determine low tilts of the lipid acyl chains from the lipid CH_2 stretching modes. (2) The amide A band in these conditions, i.e. when the sample is exposed to $^2\text{H}_2\text{O}$, originates only from the regions of the peptide that did not undergo $\text{N}-\text{H}/\text{N}-^2\text{H}$ exchange, as would be expected from the transmembrane region of the protein. Thus any contributions of extramembraneous parts is removed and what one measures is the dichroism and subsequent orientation of the transmembrane region of the sample.

The second dichroism, $\mathcal{R}_{\text{Site}_i}$, corresponds to the $^{13}\text{C}=\text{O}$ i label, which is dependent on the rotational orientation ω for this particular residue:

$$\mathcal{R}_{\text{Site}_i}(\beta, f_i, \omega) = \frac{e_z^2 \left(f_i \mathcal{K}_z(\omega) + \frac{1-f_i}{3} \right) + e_x^2 \left(f_i \mathcal{K}_x(\omega) + \frac{1-f_i}{3} \right)}{e_y^2 \left(f_i \mathcal{K}_y(\omega) + \frac{1-f_i}{3} \right)} \quad (2)$$

These two equations are not sufficient to obtain β , ω and f_i (three unknowns), therefore a second label is inserted, in a different sample, above or below the first label. As there are 3.6 residues per turn for a canonical α -helix, the increment in ω is assumed to be 100° . Thus, with the additionally labelled sample, two additional equations can be obtained, $\mathcal{R}_{\text{Helix}_j}$ and $\mathcal{R}_{\text{Site}_j}$, dependent on (β, f_j) and $(\beta, \omega + 100^\circ, f_j)$, respectively.² Solving the four equations $\mathcal{R}_{\text{Helix}_i}$, $\mathcal{R}_{\text{Helix}_j}$, $\mathcal{R}_{\text{Site}_i}$ and $\mathcal{R}_{\text{Site}_j}$ for each i and j pair, will yield β_{ij} , ω_{ij} , f_i and f_j , where β_{ij} and ω_{ij} are the results obtained from the combinations of sample i and sample j .

These non-linear equations were solved with Newton's method as implemented in the FindRoot function in Mathematica 3.0 (Wolfram Research, Champaign, USA). The final values of β and ω for a particular pair of labels (i, j) were obtained by averaging β_{ij} and ω_{ij} , respectively:

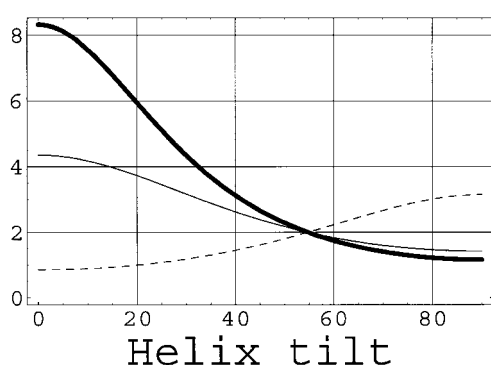


Figure 6. Possible dichroic ratios \mathcal{R} , as a function of the polymer tilt for several different α angles. Thick line, $\alpha = 29^\circ$ (amide A); thin line, $\alpha = 39^\circ$ (amide I); and broken line, $\alpha = 90^\circ$ (lipid CH_2 stretching mode). The dichroic ratios are calculated for an ATR optical geometry using the thick film approximation and a Ge internal reflection element.

$$\beta = \frac{1}{n^2} \sum_{i=1}^n \sum_{j=1}^n \beta_{ij} \quad (3)$$

$$\omega = \frac{1}{n^2} \sum_{i=1}^n \sum_{j=1}^n \omega_{ij}$$

Calculation of ω and local tilt for each labelled residue

The overall scheme by which the data were used to calculate the local helix tilt and rotational pitch angle is shown in Figure 7. Because the error in the assumption $\omega_{n+1} = \omega_n + 100$ becomes more important with the separation between residues, a first estimate of ω for a particular residue was obtained solving the equations corresponding to helix and site dichroisms only for pairs of labels separated by one ($i, i+1$) or two ($i, i+2$) residues. In these first calculations it was assumed that the difference in ω between consecutive residues is 100° although in principle this is not known.

Figure 8 shows how this was calculated. The first column in this Figure shows residues 31–51 of CD3- ζ . The second column (grey rectangle) indicates the pairwise combinations ($i, i+1$ or $i, i+2$) of labels, joined by brackets, used in the initial calculation. The result of each combination is represented by one ω angle, corresponding to the first residue in the sequence. The ω for the other label in the pair would be obviously $\omega + 100^\circ$ (for $i, i+1$) or $\omega + 200^\circ$ (for $i, i+2$). For example, ω_{V43} in the first calculation in Figure 8 is the result of combining the pair 43 and 44, whereas ω_{V44} is the result of combining 44 and 45. The fact that the combinations (43,44), (44,45) and (45,46) produced ω angles for residues 43, 44 and 45 that were separated by an increment of 100° , i.e. 120° , 222° and 331° (see Figure 8, grey rectangle), indicated that, at least for these three residues, the assumption $\omega_{n+1} = \omega_n + 100$ is a good approximation.

We then used the fact that when a good estimate for ω is obtained for a particular residue, the ω for a

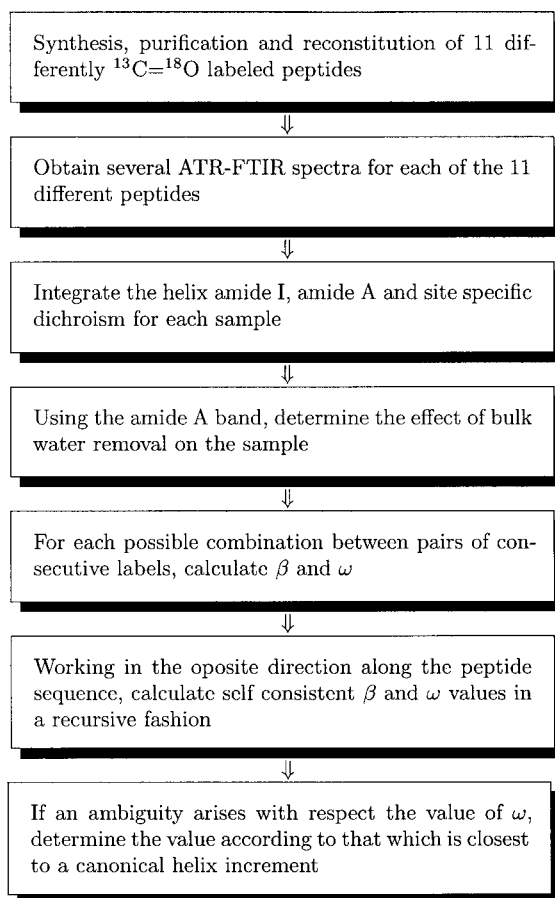


Figure 7. A scheme indicating the chronological list of events leading to the determination of the local helix tilt β and rotational pitch angle ω of the CD3- ζ transmembrane domain in this study.

different residue can be obtained without having to assume any particular value for the increment in ω between the two residues, because it can be treated as an unknown. For example, ω at residue 41 was calculated fixing the known (see above) ω at residue 43 (i.e. 120°), the four unknowns being β , ω_{41} and the f for the two samples, f_a and f_b . In Figure 8, the ω values that were fixed in the calculation are indicated by a box. Then, the ω obtained for residue 41 was fixed, and ω at residue 39 was calculated. This was propagated up and down the helix (see values to the far-right in Figure 8, so that a better estimate of ω for each residue could be obtained.

Note however, that for certain residues, e.g. 38, 39 and 46, two possible values were obtained. These two values, ~ 75 and ~ 300 for residues 38 and 46, and ~ 106 and ~ 260 for residue 39, should give identical dichroisms due to the fact that the dichroic ratio is a function of $\cos \omega$. However, only one of these values is obtained when it is assumed $\omega_{n+1} = \omega_n + 100$ (see the second column in Figure 8), which may not be a correct assumption. The other value is obtained when a good approximation for a certain residue is known, therefore we have taken the second group of ω values (see far right values in Figure 8) as correct in the subsequent calculations.

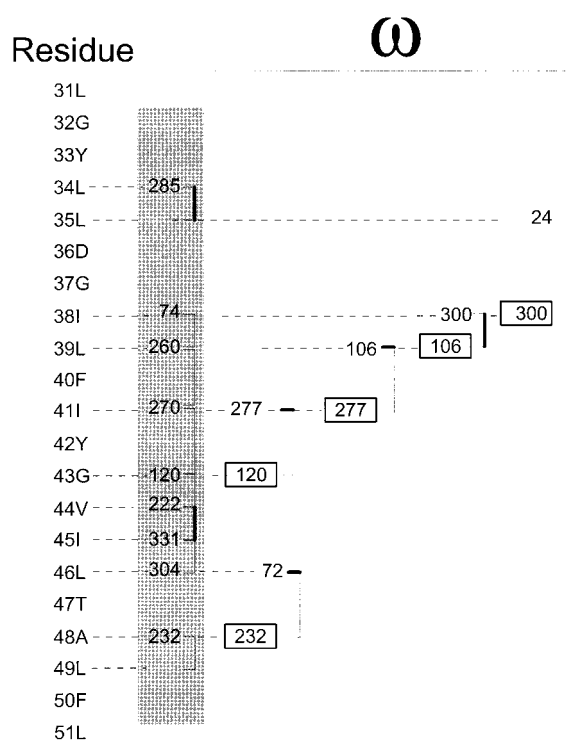


Figure 8. Scheme of the steps followed to obtain the ω angles for all the residues labelled. First, a difference of 100° between consecutive residues was assumed and the pairs used were either $(i, i + 1)$ or $(i, i + 2)$, see the grey rectangle. For each one of these combinations, the ω angle for the residue located above in the pair is indicated, e.g. for the combination of residues 43 and 44, only ω corresponding to residue 43 is shown. Second, the ω angle for certain residues were restrained to the value indicated inside a box and the ω angle of the residue linked to the box was calculated (see the text for a more detailed explanation).

Thus, the (i) ω angles obtained, (ii) the average value for the fractional sample order f_a and (iii) only the site dichroism were used to calculate the local helix tilt β .

Acknowledgement

This work was supported by grants from the Wellcome Trust and the Biotechnology and Biological Sciences Research Council to I.T.A.

References

1. Stevens, T. J. & Arkin, I. T. (2000). Do more complex organisms have a greater proportion of membrane proteins? *Protein Struct. Funct. Genet.* **39**, 417-420.
2. Arkin, I. T., MacKenzie, K. R. & Brunger, A. T. (1997). Site-directed dichroism as a method for obtaining rotational and orientational constraints

- for oriented polymers. *J. Am. Chem. Soc.* **119**, 8973-8980.
3. Torres, J., Adams, P. D. & Arkin, I. T. (2000). Use of a new label, $^{13}\text{C}=\text{O}$, in the determination of a structural model of phospholamban in a lipid bilayer. Spatial restraints resolve the ambiguity arising from interpretations of mutagenesis data. *J. Mol. Biol.* **300**, 677-685.
4. Torres, J., Kukol, A. & Arkin, I. T. (2000). The use of a single glycine residue to determine the tilt and orientation of a transmembrane helix. A new structural label for infrared spectroscopy. *Biophys. J.* **79**, 3139-3143.
5. Kukol, A., Adams, P. D., Rice, L. M., Brunger, A. T. & Arkin, I. T. (1999). Experimentally based orientational refinement of membrane protein models: a structure for the influenza A M2 H⁺ channel. *J. Mol. Biol.* **286**, 951-962.
6. Kukol, A. & Arkin, I. T. (2000). Structure of the influenza C CM2 protein transmembrane domain obtained by site-specific infrared dichroism and global molecular dynamics searching. *J. Biol. Chem.* **275**, 55-69.
7. Kukol, A. & Arkin, I. T. (1999). Structure of the HIV-1 Vpu transmembrane complex determined by site-specific FTIR dichroism and global molecular dynamics searching. *Biophys. J.* **77**, 1594-1601.
8. Torres, J., Kukol, A., Goldman, J. & Arkin, I. T. (2001). Site specific examination of secondary structure and orientation determination in membrane proteins: the peptidic $^{13}\text{C}=\text{O}$ group as a novel infrared probe. *Biopolymers*, **59**, 396-401.
9. Manolios, N. (1995). Hierarchy of T cell antigen receptor assembly. *Immunol. Cell Biol.* **73**, 544-548.
10. Jacobs, H. (1997). Pre-TCR/CD3 and TCR/CD3 complexes: decamers with differential signalling properties? *Immunol. Today*, **18**, 565-569.
11. Caplan, S. & Baniyash, M. (2000). Searching for significance in TCR-cytoskeleton interactions. *Immunol. Today*, **21**, 223-228.
12. Rutledge, T., Cosson, P., Manolios, N., Bonifacino, J. S. & Klausner, R. D. (1992). Transmembrane helical interactions: zeta chain dimerization and functional association with the T cell antigen receptor. *EMBO J.* **11**, 3245-3254.
13. Bolliger, L. & Johansson, B. (1999). Identification and functional characterization of the zeta-chain dimerization motif for TCR surface expression. *J. Immunol.* **163**, 3867-3876.
14. Wellings, D. A. & Atherton, E. (1997). Standard Fmoc protocols. *Methods Enzymol.* **289**, 44-67.
15. Briggs, J. A. G., Torres, J. & Arkin, I. T. (2001). A new method to model membrane protein structure based on silent amino-acid substitutions. *Proteins: Struct. Funct. Genet.* **44**, 370-375.
16. Tsuboi, M. (1962). Infrared dichroism and molecular conformation of α -form poly-g-benzyl-L-glutamate. *J. Polym. Sci.* **59**, 139-153.
17. Marsh, D., Muller, M. & Schmitt, F. J. (2000). Orientation of the infrared transition moments for an α helix. *Biophys. J.* **78**, 2499-2510.
18. Harrick, N. (1967). *Internal Reflection Spectroscopy*, 1st edit., Interscience Publishers, New York.
19. Byler, D. & Susi, H. (1986). Examination of the secondary structure of proteins by deconvolved FTIR spectra. *Biopolymers*, **25**, 469-487.
20. Torres, J., Briggs, J. A. G. & Arkin, I. T. (2002). Convergence of experimental and

evolutionary approaches predicts the presence of a tetrameric form for CD3- ζ . *J. Mol. Biol.* **316**, 375-384.

21. Kraulis, P. (1991). MOLSCRIPT: a program to produce both detailed and schematic plots of protein structures. *J. Appl. Crystallog.* **24**, 946-950.

Edited by W. Baumeister

(Received 18 May 2001; received in revised form 3 October 2001; accepted 31 October 2001)